DEVELOPMENT AND VERIFICATION OF A NON-LINEAR LOOK-UP TABLE MODEL FOR MOSFETS

D. Schreurs, E. Vandamme*, C. van Dinther**

K.U.Leuven, Div. ESAT-TELEMIC, Kardinaal Mercierlaan 94, B-3001 Leuven, Belgium
E-mail: dominique.schreurs@esat.kuleuven.ac.be, Fax: +32-16-321986, Phone: +32-16-321821
*IMEC, Div. STDI/CMOS, Kapeldreef 75, B-3001 Leuven, Belgium
**Philips Semiconductors, Gerstweg 2, NL-6534 AE Nijmegen, The Netherlands

ABSTRACT

The non-linear behaviour of MOSFETs is historically represented by compact models. Now that MOSFETs are gradually used in high-frequency analogue circuits, techniques originally developed for III-V devices can be applied and adjusted to MOSFETs. We present the development of an accurate table-based MOSFET model and stress the differences with the corresponding HEMT implementation.

INTRODUCTION

The performance and yield of silicon technologies have reached the level of system-on-chip realisation. This trend stresses the need for efficient and accurate non-linear MOSFET modelling to minimise the design cycles of analogue circuits. The non-linear behaviour of MOSFETs was in the past mainly described by compact models, such as the BSIM3 model (1), or more recently by empirical models, such as (2). These approaches are historically driven by the need to be SPICE compatible. Nowadays, more and more microwave design techniques enter the era of silicon analogue circuit design. Therefore it is advisory to evaluate typical III-V compounds modelling techniques for MOSFETs. In this work, we present a procedure to determine a look-up table MOSFET model. An important difference with compact models is that the proposed model is based on high-frequency S-parameter measurements and not on DC and low-frequency C-V measurements, which could hide particular HF problems, such as dispersion. A second difference is that there is only one device to be measured, in contrary to several devices with various dimensions in case of compact models.

A look-up table model representation means that the device's state functions, i.e., the charge and current sources, are tabulated as function of the terminal voltages. These state functions are obtained by integrating the bias-dependent intrinsic elements of the transistor. The non-linear model is completed by incorporating lumped components which represent the bias-independent extrinsic elements. We first focus on the determination of the small-signal equivalent circuit. Subsequently, we discuss the non-linear model and evaluate its accuracy by comparing simulations with vectorial large-signal measurements.

NON-LINEAR MODELLING PROCEDURE

The MOSFET belongs to the field-effect device family, which means that the small-signal and large-signal equivalent circuit topologies are similar to those of MESFETs and HEMTs (Figures 1 and 2 left). Therefore, an important difference in the non-linear modelling procedures for different FET types lies in the determination of the access elements. We make a clear distinction between, on one hand, the bonding pads and access transmission lines and, on the other hand, the extrinsic, parasitic device elements, because the aim is to derive a model for a device as it would be inserted in an actual circuit.

The first step in the modelling procedure is hence the de-embedding of the access transmission lines. Due to the low-resistivity of standard silicon substrates, these transmission lines are strongly dispersive. Since EM simulators are time-consuming and not yet provide the required accuracy for this kind of structures, on-wafer calibration is often preferred. The drawback is that special passive structures need to be foreseen on the mask set. In this work, we applied the three-step de-embedding method (3) to move the reference plane from the probe tips to the device.

Subsequently, the extrinsic elements have to be determined. A wide-spread procedure for MESFETs is the cold method developed by Dambrine *et al.* (4). This method requires a non-negligible gate-current to extract the extrinsic resistances and inductances. Because HEMTs already start to degrade at the required gate current level, we proposed earlier a modified cold method (5) to overcome this condition. As the gate current level of MOSFETs is very small, the modified cold method should be used. We obtained by this method values for the gate, drain, and source resistances that are consistent with the physically known square resistances of the ohmic contacts and gate metallisation. The values for the extrinsic capacitances and inductances were small and not clearly defined. We think that this is due to the three-step de-embedding method, because it is difficult to design adequate passive structures that result in a clear separation between the device and access parts. A possible solution is to consider other on-wafer calibration methods, like multi-line techniques.

After de-embedding the extrinsic part, the bias-dependent intrinsic elements can be extracted. To have a consistent transition between the small-signal and large-signal equivalent schemes, we have taken the small-signal equivalent circuit topology of (6) (Figure 2 right). Its basic principle is that the feedback capacitance C_{gd} is replaced by a transcapacitance at both the gate and drain. The maximum error made by converting the 'conventional' equivalent scheme to this 'modified' topology increases with frequency and is for the investigated MOSFETs less than 1% at 50 GHz. As for HEMTs, there exist optimal frequency bands over which the intrinsic elements are extracted. We found that all elements can accurately be extracted at frequencies up to 5 GHz, except for the charging resistance R_i and the drain-source capacitance C_{dsi}, for which a minimum extraction frequency of 10 GHz is recommended. To determine the bias-dependency of the intrinsic elements, S-parameter measurements are performed at multiple bias points. The bias steps depend on the application. If the model is aimed for use in the saturation region, the typical step sizes are 50 mV for V_{gs} and 100 mV for V_{ds}. In case of a cold application, such as a resistive mixer, a denser (e.g., 20 mV) and also negative V_{ds} grid is required.

The final step in the non-linear modelling procedure is the integration of the bias-dependent intrinsic elements towards the corresponding terminal voltages:

$$Q_{gs}\left(V_{gsi},V_{dsi}\right) = \int_{V_{gsi0}}^{V_{gsi}} C_{gi}\left(V,V_{dsi0}\right)dV + \int_{V_{dsi0}}^{V_{dsi}} C_{dm}\left(V_{gsi},V\right)dV \quad (1)$$

$$Q_{ds}\left(V_{gsi},V_{dsi}\right) = \int_{V_{gsi0}}^{V_{gsi}} C_{m}\left(V,V_{dsi0}\right)dV + \int_{V_{dsi0}}^{V_{dsi}} C_{dsi}\left(V_{gsi},V\right)dV \quad (2)$$

$$I_{ds}\left(V_{gsi},V_{dsi}\right) = I_{ds}\left(V_{gsi0},V_{dsi0}\right) + \int_{V_{gsi0}}^{V_{gsi}} g_{mi}\left(V,V_{dsi0}\right)dV + \int_{V_{dsi0}}^{V_{dsi}} g_{dsi}\left(V_{gsi},V\right)dV \quad (3)$$

where the index i denotes the internal gate- and drain voltages and V_{gsi0}, V_{dsi0} the starting point for the integration. A noticeable difference between MOSFETs and HEMTs (7) is the larger contribution of the MOSFET feedback capacitance C_{gd} ($C_{dm} \approx C_m \approx -C_{gd}$) to the charge sources. The reason is that the MOSFET gate is self-aligned between source and drain, whereas HEMTs are typically processed with the gate offset towards the source to decrease C_{gd} and the source resistance. Finally, the obtained look-up table model can be implemented in microwave circuit simulators supporting this type of customised models.

NON-LINEAR MODEL VERIFICATION

The developed procedure has been applied to a 36-finger nMOSFET (8) with a channel length of 0.18 μm and a total gate width of 146 μm. We first compared S-parameter simulations with measurements at different operating conditions to check the bias-dependent small-signal extractions. Non-linear models only can be fully verified by *vectorial* large-signal measurements (9), which means that not only the accuracy of the simulated magnitude but also that of the phase of the spectral components of voltages and currents can be evaluated. It has to be noted that, in a way similar to the de-embedding of the S-parameter measurements, the reference plane of the large-signal measurements has to be shifted to the device plane by applying the three-step de-embedding method. Figure 3 shows the very good agreement between the measured and simulated first three harmonics of the output power. An advantage of the measurement set-up is that models also can be verified under multi-tone excitations. This is shown in Figure 4, which presents the well modelled time-domain waveforms of the terminal voltages and currents. The transition between the linear and saturation regime (Figure of V_{ds}(t)) can still be improved by decreasing the V_{ds} step at which measurements are taken around the knee voltage.

CONCLUSIONS

We developed a large-signal look-up table model for MOSFETs. We pointed out that the basic procedure is similar to that of HEMTs, but that special attention has to be paid to the accurate de-embedding of the dispersive silicon access transmission lines. The non-linear model, being verified by the novel vectorial large-signal measurement technique, is shown to be accurate in both time and frequency domain.

ACKNOWLEDGEMENTS

The authors acknowledge Agilent Technologies for the NNMS donation. This work was supported by the IWT and the Belgian program on interuniversity attraction poles (IUAP-IV/2). D. Schreurs is supported by the Fund for Scientific Research-Flanders as a post-doctoral fellow.

REFERENCES

(1) W. Liu *et al.*, “BSIM3v3.2 MOSFET Model Users’ Manual”, 1998, University of California, Berkeley.
(2) C. Biber *et al.*, “A Nonlinear Microwave MOSFET Model for Spice Simulators”, 1998, *IEEE Trans. Microwave Theory Techn.*, Vol. 46, No. 5, pp. 604–610.
(3) H. Cho and D.E. Burk, “A three step method for the de-embedding of high frequency S-parameter measurements”, 1991, *IEEE Trans. Electron Devices*, Vol. 38, No. 6, pp. 1371–1375.
(4) G. Dambrine *et al.*, “A New Method for Determining the FET Small-Signal Equivalent Circuit”, 1988, *IEEE Trans. Microwave Theory Techn.*, Vol. 36, No. 7, pp. 1151–1159.
(5) D. Schreurs *et al.*, “S-Parameter Measurement Based Quasi-Static Large-Signal Cold HEMT Model For Resistive Mixer Design”, 1996, *Int. J. Microwave and Millimeter-Wave Computer-Aided Engineering*, Vol. 6, No. 4, pp. 250–258.
(6) Ph. Jansen *et al.*, “Consistent Small-Signal and Large-Signal Extraction Techniques for Heterojunction FETs”, 1995, *IEEE Trans. Microwave Theory Techn.*, Vol. 43, No. 1, pp. 87–93.
(7) D. Schreurs *et al.*, “Improved HEMT model for low phase noise InP based MMIC oscillators”, 1998, *IEEE Trans. Microwave Theory Techn.*, Vol. 46, No. 10, pp. 1583–1585.
(8) E. Augendre *et al.*, “A high performance 0.18 μm elevated source/drain technology with improved manufacturability”, 1999, *Proc. 29th European Solid-State Device Research Conference*, pp. 636–639.
(9) J. Verspecht *et al.*, “Accurate On Wafer Measurement Of Phase And Amplitude Of The Spectral Components Of Incident And Scattered Voltage Waves At The Signal Ports Of A Nonlinear Microwave Device”, 1995, *IEEE MTT-S Int. Microwave Symp. Digest*, pp. 1029–1032.

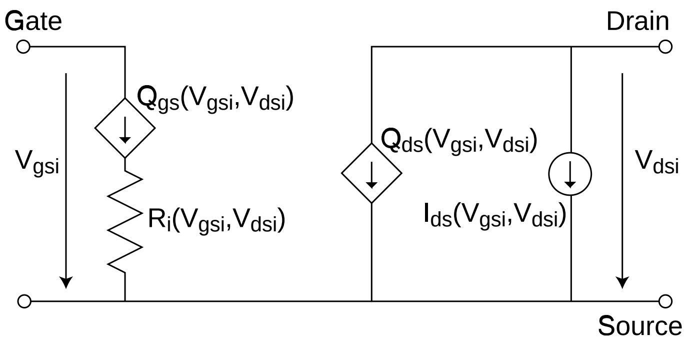

Figure 1: Intrinsic non-linear MOSFET model. Compared to the usual MESFET/HEMT topologies, I_{gs} can be omitted.

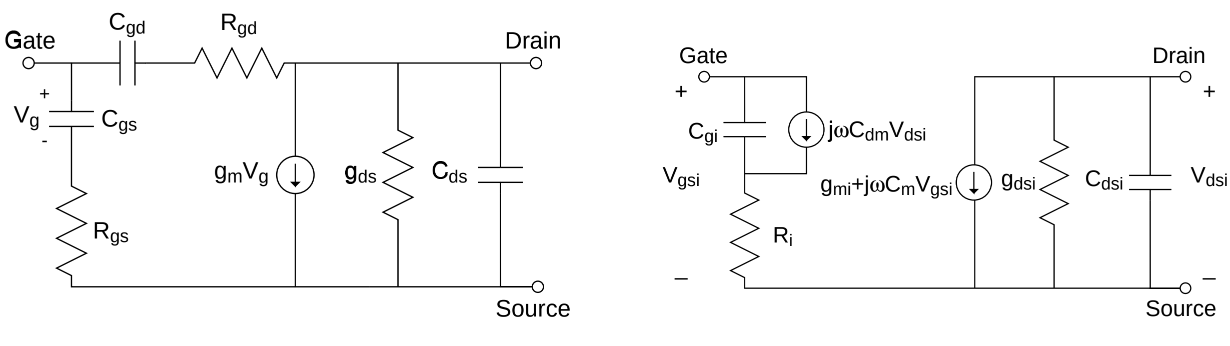

Figure 2: Intrinsic small-signal equivalent scheme of the MOSFET with conventional topology (left) and modified topology (right).

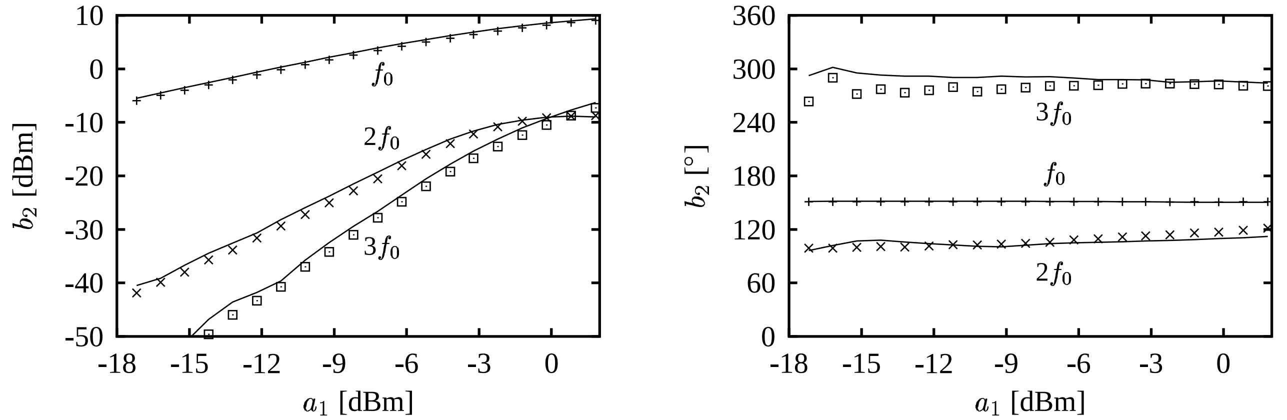

Figure 3: Measured and simulated (__) magnitude (left) and phase (right) of the first three harmonics of the output power of a 0.18 μm x 146 μm nMOSFET (V_{gsDC}= 0.6 V, V_{dsDC}= 1.2 V, f_0= 3.6 GHz).

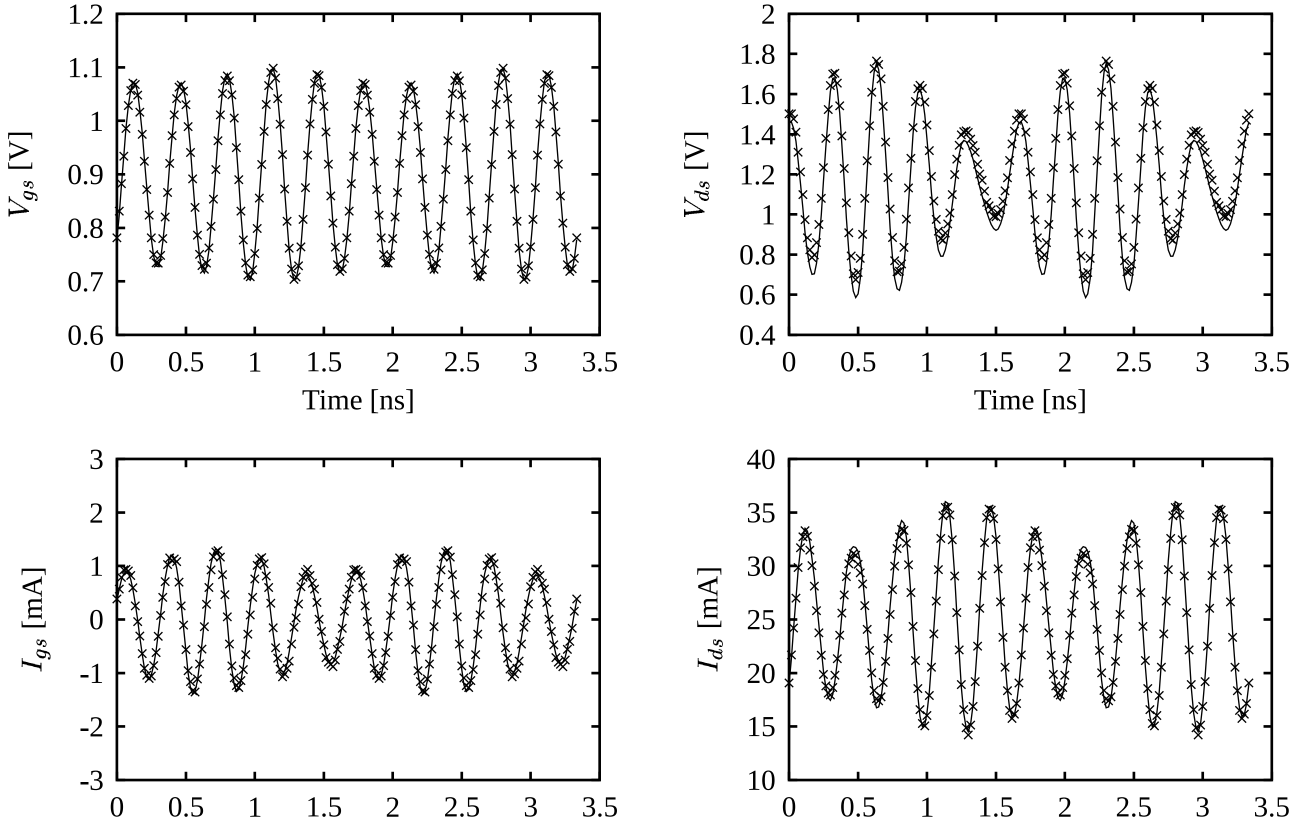

Figure 4: Measured (x) and simulated (__) time domain waveforms of the terminal currents and voltages of a 0.18 μm x 146 μm nMOSFET (V_{gsDC}= 0.9 V, V_{dsDC}= 1.2 V, f_1= 3 GHz, a_1= -10 dBm, f_2= 3.6 GHz, a_2= -7 dBm, $\phi\left(a_2\right) - \phi\left(a_1\right)$= 37°).